AIP | Applied Physics Letters

Interface modification for highly efficient organic photovoltaics

Roland Steim, Stelios A. Choulis, Pavel Schilinsky, and Christoph J. Brabec

Citation: Appl. Phys. Lett. **92**, 093303 (2008); doi: 10.1063/1.2885724
View online: http://dx.doi.org/10.1063/1.2885724
View Table of Contents: http://apl.aip.org/resource/1/APPLAB/v92/i9
Published by the American Institute of Physics.

Interface modification for highly efficient organic photovoltaics

Roland Steim,[1,2] Stelios A. Choulis,[1,a),b)] Pavel Schilinsky,[1] and Christoph J. Brabec[1,a),c)]
[1]*Konarka Technologies GmbH, Landgrabenstr. 94, D-90443 Nürnberg, Germany*
[2]*Light Technology Institute, Universität Karlsruhe (TH), Kaiserstr. 12, D-76131 Karlsruhe, Germany*

(Received 11 December 2007; accepted 5 February 2008; published online 4 March 2008)

We present highly efficient inverted polymer:fullerene bulk-heterojunction solar cells by incorporation of a nanoscale organic interfacial layer between the indium tin oxide (ITO) and the metal oxide electron-conducting layer. We demonstrate that stacking of solution-processed organic and metal oxide interfacial layers gives highly charged selective low ohmic cathodes. The incorporation of a polyoxyethylene tridecyl ether interfacial layer between ITO and solution-processed titanium oxide (TiO_x) raised the power conversion efficiency of inverted organic photovoltaics to 3.6%, an improvement of around 15% in their performance over comparable devices without the organic interfacial layer. © *2008 American Institute of Physics*.
[DOI: 10.1063/1.2885724]

During the past decade, there has been an intensive search for cost-effective photovoltaics.[1,2] Among all alternative technologies to inorganic solar cells, polymer solar cells have the potential for the most significant cost reduction since they can be printed at low temperatures on flexible substrates.[3] At present, bulk-heterojunction structures based on blends of regioregular poly(3-hexylthiophene) RR-P3HT, and a highly soluble fullerene derivative ([6,6]-phenyl-C61-butyric acid methyl ester) PCBM, have been among the material systems with the highest reported efficiencies.[4,5]

For the superstrate device architecture, solar cells based on glass/indium tin oxide(ITO)/poly(3,4-ethylenedioxythiophene) (PEDOT):poly(styrene-sulfonate) (PSS)/RR-P3HT:PCBM/Al, power conversion efficiencies (PCEs) in the range of 4%–4.5% have been reported.[4,5] These PCE values were much higher compared to that reported for RR-P3HT:PCBM in the substrate ("inverted") architecture.[6–9] The development of highly efficient inverted solar cells is an interesting architecture since it allows us to study fundamental processes in bulk-heterojunction architecture, including the vertical phase segregation of polymer/fullerene composites as well as the charge selectivity of the interfacial contacts.[10] Another potential advantage of this technology is its more natural compatibility with metal grid electrodes, which may become a likely replacement for ITO-based electrodes. Thus, identification of engineering methods to further improve the PCE of the inverted solar cells is of relevance.

Previous attempts to make bulk-heterojunction organic solar cells with inverted layers have resulted in device performance which was below the state of the art performance of the superstrate architecture (PCE of less than 3% was achieved).[6–9] One of the main challenges of inverted solar cells is the high charge selectivity for electron extraction at the bottom electrode. We have recently reported on solution-processed titanium oxide (TiO_x) as a highly charge selective interfacial layer. Solution processing of TiO_x on top of ITO gave fairly optimized charge selectivity and allowed to manufacture inverted organic solar cells with a PCE of up 3.1%.[10] In our previously reported inverted structure glass/ITO/TiO_x/RR-P3HT:PCBM/PEDOT:PSS/Au, the electrons are extracted at the bottom electrode (ITO/TiO_x) and the holes are extracted at the top electrode (PEDOT:PSS/Au).[10]

In this letter, we report further performance improvement of inverted solar cells by incorporating an interfacial layer between ITO and TiO_x to improve the quality of the TiO_x electron extraction layer. The new proposed structure is based on glass/ITO/interfacial layer/TiO_x/PR-P3HT:PCBM/PEDOT:PSS/Ag (see Fig. 1). The replacement of top metal electrode from Au to a higher reflective metal such as Ag is expected to give lower absorption losses at the top electrode.

The photoactive layer of the devices is a blend of RR-P3HT:PCBM in *o*-xylene sandwiched between the two extracting electrodes. Devices were processed as reported earlier[10] and measured with and without the influence of ultraviolet (UV) light. The current density–voltage (*J-V*) characteristics were measured with a Keithley source measurement unit (SMU 2400). For illumination, a calibrated Steuernagel solar simulator was used providing an AM 1.5G spectra at 100 mW/cm^2. The Steuernagel solar simulator is equipped with metal halogenide lamps. The mismatch factor

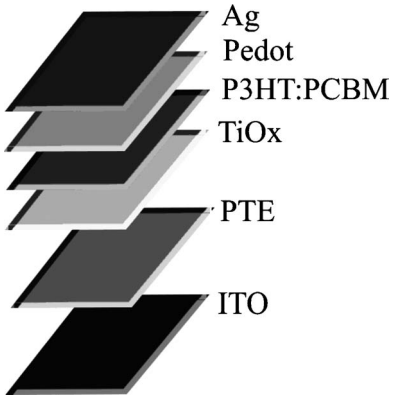

FIG. 1. Device structure of the inverted solar cell using stacking of solution-processed organic (PTE) and metal oxide (TiO_x) interfacial layers as electron selective bottom contact.

[a)]Authors to whom correspondence should be addressed.
[b)]Present address: Department of Mechanical Engineering and Materials Science and Engineering, Cyprus University of Technology, 3603 Limassol, Cyprus. Electronic mail: stelios.choulis@cut.ac.cy.
[c)]Electronic mail: cbrabec@konarka.com.

of the solar simulator to P3HT:PCBM based solar cells was assesed by cross calibrating to external quantum efficiency measurements. A mismatch factor of 0.75 was determined. All efficiency performance values in this paper have been calculated using a mismatch of 0.75.

The solar cells under investigation had a typical active area of 20 mm^2. The active area of the devices was defined by scribing the hole conducting layer along the outline of the Ag electrode. This patterning step is required to suppress artificial photocurrent contributions from outside the active device area, i.e., preventing lateral current collection via the hole conducting buffer layer. Due to the tolerances in the mechanical patterning process, we estimate an uncertainty of up to 5% in the determination of the active area. That may lead to an efficiency overestimation by a similar amount.

In the present study, polyoxyethylene tridecyl ether (PTE) [$C_{13}H_{27}(OCH2CH2)_{12}OH$, Aldrich] was used as an organic interfacial layer to improve the quality of the TiO_x layer (see Fig. 1). The organic interfacial layer (0.1 wt % in water) was doctor bladed onto the glass/ITO substrate and resulted to an ultrathin layer with an estimated thickness of less than 10 nm.

The device architectures studied are summarized as follows. Our control devices based on TiO_x interfacial layer as electron selective contact (glass/ITO/TiO_x/PR-P3HT:PCBM/PEDOT:PSS/Ag) are compared with device architectures which had PTE interfacial layer between the ITO and the TiO_x electron selective contact (glass/ITO/PTE/TiO_x/PR-P3HT:PCBM/PEDOT:PSS/Ag). Finally, both sets of devices are compared to solar cells without any electron selective layer at all (glass/ITO/RR-P3HT:PCBM/PEDOT:PSS/Ag).

Figure 2 shows the representative *J-V* measurements of the solar cells in the dark (upper plot) and under illumination (lower plot). The *J-V* data under illumination are measured with and without the influence of UV light. Similar to previous observations, we have observed an increase in the device performance when UV light is present.[11] We will discuss this point in more details in a separate publication.

The dark *J-V* curve for the inverted solar cell without an electron selective interfacial layer (glass/ITO/RR-P3HT:PCBM/PEDOT:PSS/Ag) shows low current in the forward direction and a high leakage current in the reverse direction. It is clear that ITO alone does not provide an electron selective contact for the extraction of electrons and blocking of holes. By using low temperature solution-processed TiO_x (glass/ITO/TiO_x/RR-P3HT:PCBM/PEDOT:PSS/Ag) as interfacial layer, the electron selectivity of the bottom contact improves significantly. A high current in the forward direction as well as low leakage currents are achieved. The improved carrier selectivity is also reflected in the fill factor (FF) of the corresponding cells in the light *J/V* data (see Fig. 2, lower plot).

The best selectivity (highest injection current and low leakage current) is observed for solar cells using a combination of PTE and TiO_x (glass/ITO/PTE/TiO_x/RR-P3HT:PCBM/PEDOT:PSS/Ag). This is also followed from a detailed analysis of the *J-V* curves according to the one-diode model.[12] The insertion of a thin PTE layer (glass/ITO/PTE/TiO_x/RR-P3HT:PCBM/PEDOT:PSS/Ag) reduces the serial resistance of the glass/ITO/TiO_x/RR-P3HT:PCBM/PEDOT:PSS/Ag solar cells from 3 to 1 Ω and increases the shunt resistance from 14 to 31 kΩ. The combination of reduced serial resistance and increased shunt resistance is reflected in the higher FF observed for these diodes.

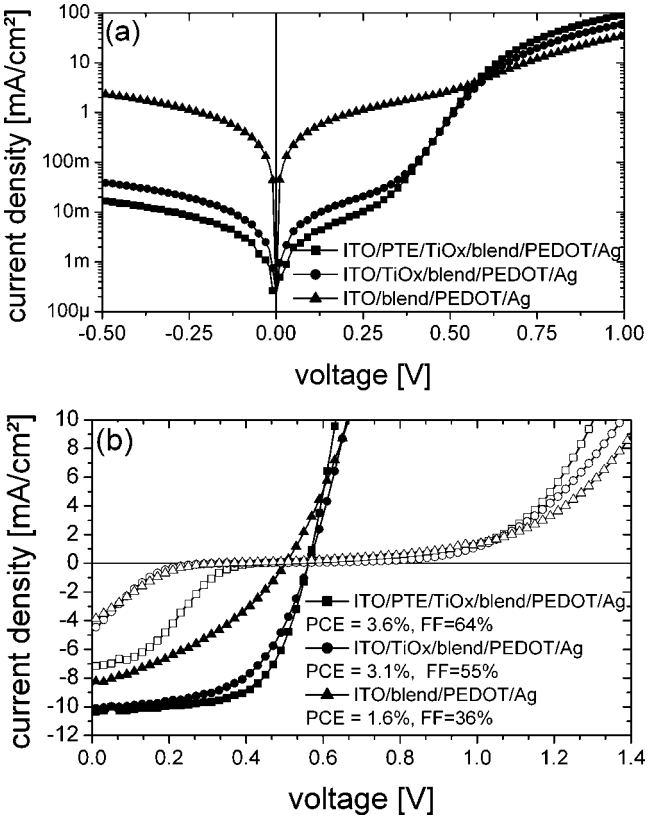

FIG. 2. Upper plot (a) representative dark current density–voltage characteristics of the solar cells under study in the voltage range representing the opening of the diode. The data are plotted in a logarithmic-linear plot representation. Bottom plot (b) current density–voltage characteristics of the solar cells studied under illumination with UV light illumination (filled symbols) and without UV illumination (open sympols).

Figure 3 summarize the performance parameters of the solar cells studied under UV illumination. Data are presented

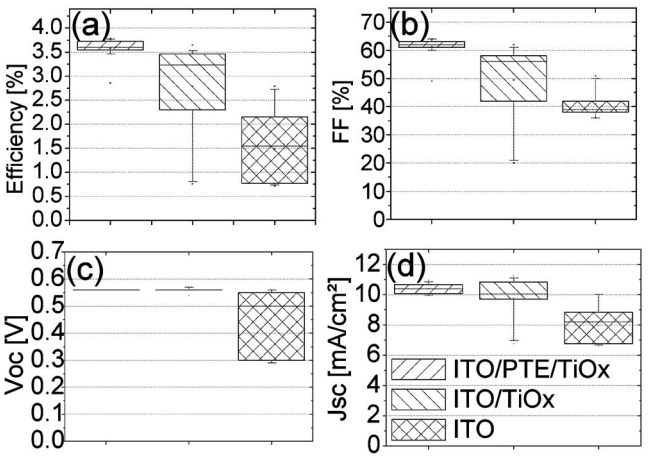

FIG. 3. Comparison of the (a) power conversion efficiency, (b) fill factor (FF), (c) open circuit voltage (V_{OC}), and (d) short circuit current density (J_{SC}) for the solar cells under study. Data are presented in box plots. The horizontal lines in the box denote the 25th, 50th, and 75th percentile values. The error bars denote the 5th and 95th percentile values. The two symbols below and above the 5th/95th percentile error bar denote the highest and the lowest observed values, respectively. The open square inside the box denotes the mean value. The height of the box is the measure for the tolerance.

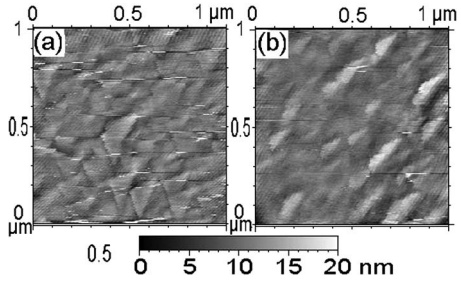

FIG. 4. Topographic atomic force microscope image (contact mode) of the TiO_x surface when is coated on the top of ITO (a) and on the top of PTE (b). The scan range was 1 μm−1 μm−20 nm.

in box plots (see Fig. 3). Three series of cells [without electron selective layer (ITO), with TiO_x electron selective contact (ITO/TiO_x), and with a combination of PTE and TiO_x (ITO/PTE/TiO_x) with 16 solar cells each were investigated. The 50% of the cells with TiO_x electron selective contact have a PCE of 3.2% or higher, a value which is slightly better compared to our previous published data based on a similar structure.[10] As discussed in the introduction, we attribute the small improvement in performance to the higher reflectivity of the Ag back electrode compared to an Au back electrode. Solar cells without any electron selective layer have a median PCE in the range of 1.6%. The best device performance was achieved with a combination of PTE and TiO_x as electron selective contact, with 50% of the cells having a PCE higher than 3.6%. We note that the data presented here have been collected from the same experimental run but were confirmed and reproduced in several other independent runs.

Since the PTE is an ultrathin, insulating layer is not a functional layer but a passive layer. The electron selective layer of the ITO/PTE/TiO_x/RR-P3HT:PCBM/PEDOT:PSS/Ag device is still the TiO_x layer. To further investigate the effect of PTE interfacial layer on ITO/PTE/TiO_x interface, we performed photogenerated-current-voltage measurements as described in detail elsewhere[13] of the solar cells under study to investigate changes in the built in voltage (V_{bi}) by PTE interface modification. The photogenerated-current-voltage measurements identified no difference in V_{bi} for the devices using ITO/TiO_x and ITO/PTE/TiO_x as electron selective contact. For both cases, the V_{bi} was found to be 0.64 V, thus the interface modification does not alter the work function of the bottom electrode.[14]

Thus, the underlying mechanism of the improved electron selectivity by incorporation of PTE in the ITO/TiO_x interface (ITO/PTE/TiO_x/RR-P3HT:PCBM/PEDOT:PSS/Ag organic photovoltaics) can be related to an improvement of the overall surface quality (roughness and/or surface energy) of the ITO/PTE/TiO_x bottom electrode. Indications that the surface morphology of the TiO_x is altered when coated on the top of PTE compared to ITO are found from atomic force microscopy studies (Fig. 4). Although the surface rougness of the TiO_x coated on the top of ITO and PTE has the same rms value of 2.2 nm, the distance between the peaks and valleys is different. We attributed the improvement in the electron selectivity of the ITO/PTE/TiO_x bottom electrode to PTE coating step, allowing better wetting of the TiO_x precursor solution. Excellent wetting of the TiO_x layer is essential to guarantee homogenous hydrolysis and electrode properties and can also provide more intimate interface with the photoactive layer.

In summary, we presented a detailed study on the role of stacking solution-processed organic and metal oxide interfacial layers, PTE interfacial layer on the device performance of inverted bulk heterojunction polymer:fullerene based solar cells. PTE interface modification clearly alters the functionality of the electron selective bottom electrode (ITO/PTE/TiO_x). The improved selectivity of the electron selective bottom contact with the incorporated PTE interfacial layer between ITO and TiO_x is reflected in the FF values of the corresponding solar cell device. Due to better electron selectivity, better FF value is achieved. By incorporating a PTE interfacial layer between ITO and TiO_x, a PCE of 3.6% for inverted bulk-heterojuction polymer:fullerene solar cells has been achieved.

[1] C. J. Brabec, J. A. Hauch, P. Schilinsky, and C. Waldauf, MRS Bull. **30**, 50 (2005).
[2] N. S. Sariciftci, L. Smilowitz, A. J. Heeger, and F. Wudl, Science **258**, 1474 (1992); J. J. M. Halls, C. A. Walsh, N. C. Greenham, E. A. Marseglia, R. H. Friend, S. C. Moratti, and A. B. Holmes, Nature (London) **376**, 498 (1995); G. Yu, J. Gao, J. C. Hummelen, F. Wudl, and A. J. Heeger, Science **270**, 1789 (1995).
[3] C. Hoth, S. A. Choulis, P. Schilinsky, and C. J. Brabec, Adv. Mater. (Weinheim, Ger.) **19**, 3973 (2007).
[4] Y. Kim, S. Cook, S. M. Tuladhar, S. A. Choulis, J. Nelson, J. R. Durrant, D. D. C. Bradley, M. Giles, I. McCulloch, C. S. Ha, and M. Ree, Nat. Mater. **5**, 197 (2006).
[5] W. Ma, C. Yang, X. Gong, K. Lee, and A. J. Heeger, Adv. Funct. Mater. **18**, 572 (2006); G. Li, V. Shrotriya, J. Huang, Y. Yao, T. Moriarty, K. Emery, and Y. Yang, Nat. Mater. **4**, 864 (2005); S. Curran and D. L. Carroll, Org. Lett. **7**, 5749 (2005).
[6] Y. Salin, S. Alem, R. de Bettignies, and J.-M. Nunzi, Thin Solid Films **476**, 340 (2005).
[7] M. Glatthaar, M. Niggemann, B. Zimmermann, P. Lewer, M. Riede, A. Hinsch, and J. Luther, Thin Solid Films **491**, 298 (2005).
[8] G. Li, C.-W. Chu, V. Shrotriya, J. Huang, and Y. Yang, Appl. Phys. Lett. **88**, 253503 (2006).
[9] M. S. White, D. C. Olson, S. E. Shaheen, N. Kopidakis, and D. S. Ginley , Appl. Phys. Lett. **89**, 143517 (2006).
[10] C. Waldauf, M. Morana, P. Denk, P. Schilinsky, K. Coakley, S. A. Choulis, and C. J. Brabec, Appl. Phys. Lett. **89**, 233517 (2006).
[11] J. Gilot, M. M. Wienk, and R. A. J. Janseeb, Appl. Phys. Lett. **90**, 143512 (2007).
[12] C. Waldauf, M. C. Scharber, P. Schilinsky, J. A. Hauch, and C. J. Brabec, J. Appl. Phys. **99**, 104503 (2006).
[13] P. Schilinsky, Ph.D. thesis, University of Oldenburg, 2005.
[14] S. A. Choulis, V.-E. Choong, A. Patwardhan, M. K. Mathai, and F. So, Adv. Funct. Mater. **16**, 1075 (2006).